EM-Neuro Modeling Across Scales for Bioelectronic Medicine

Lecture 7: Morphology, synapses, microcircuits; point vs. spiking networks

Esra Neufeld[*] and Taylor Newton[*†]

[*]IT'IS Foundation for Research on Information Technologies in Society

[†]Integrated Systems Laboratory, ETH Zurich

The Story Arc: Why This Lecture?

- Weeks 1–6: ion channels → axons → volume conductors → SCS… what about the choice of scale itself?
- **Central question:** When does morphological detail matter, and when can do without? Depends on the question:
  - ***Which* neural element does an electrode activate?** → requires spatial detail
  - ***How does* a circuit respond to activation?** → often captured by simpler models
- Today's content in four parts:
  - **Dendrites & synapses** — establish what morphological detail buys us (and what depends on synapse location)
  - **Microcircuit motifs** — how E/I populations interact; emergent dynamics arise from connectivity
  - **Simplification** — BBP's 31,000-neuron pipeline quantifies what survives/what is lost when detailed neurons become points
  - **DBS application** —clinical case where both scales are needed: spatial models for activation, simplified models for network dynamics

- Unifying principle: **match model complexity to the question at hand**

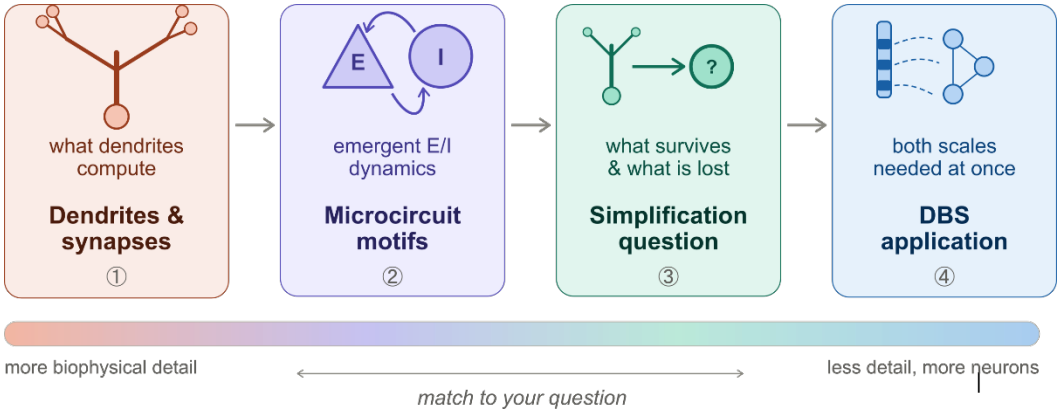

Outline for Today

- Dendritic Computation — Cable equation, compartmental models, active dendrites
- Synaptic Mechanisms — TM model, receptor kinetics, E/I balance
- Microcircuit Motifs — Canonical circuits, FFI/FBI, Brunel's phase diagram
- The Simplification Question — Point neuron zoo, BBP pipeline case study
- DBS Circuit Motifs — Two-scale modeling, basal ganglia networks, adaptive DBS
- Exercise Preview — Mini project work

Course Outline

DATE	LECTURE THEME
19.02	Motivation, logistics & tooling (EN, TNE)
26.02	Ion channels & membranes (EN)
05.03	Axon models, activating functions & electrical stimulation (EN)
12.03	EM field simulation fundamentals & coupled EM-neuro workflows (EN)
19.03	Peripheral nerves & interfaces for bioelectronic medicine (EN)
26.03	Spinal cord stimulation for neuroprosthetics and pain management & low-frequency exposure safety (TNE)
02.04	Morphology, synapses, microcircuits; point vs spiking networks (TNE)
09.04	No class: Easter break
16.04	Neural mass & whole brain models; hybridization (TNE)
23.04	Recording modalities, signal content & the reciprocity theorem (TNE)
30.04	Non invasive brain stimulation & temporal interference (TNE)
07.05	Image based/personalized treatment planning and optimization (EN)
14.05	No class: Ascension Day
21.05	Verification, validation, UQ, and reproducibility (EN)
28.05	Project presentations & synthesis (EN, TNE)

Room: ETZ E7

13:15-14:00 Lecture

14:00-14:15 Break

14:15-15:00 Lecture

14:00-14:15 Break

15:15-16:00 Exercise

Recorded Lectures & Course Material

Provided Here

Exercise Outline

DATE	EXERCISE THEME
19.02	"Hello Neuron": integrate-and-fire in Python/NEURON
26.02	Point neuron phase portrait; basic time integration numerics
05.03	Recruitment prediction for myelinated axon using AF/GAF
12.03	EM (FEM) modeling of transcranial brain stimulation
19.03	Stimulation selectivity and signal content modeling for nerve interfaces
26.03	Guest (SCS – NeuroRestore)
02.04	Mini project work
09.04	No class: Easter break
16.04	Guest (Neuromodulation Spin-Off – Z43)
23.04	Mini project work
30.04	Guest (NIBS – Kinderspital)
07.05	Mini project work
14.05	No class: Ascension Day
21.05	Mini project work
28.05	Project presentations

Room: ETZ E7

13:15-14:00 Lecture

14:00-14:15 Break

14:15-15:00 Lecture

14:00-14:15 Break

15:15-16:00 Exercise

Learning Objectives

- Derive the cable equation from first principles and explain how the length constant λ and time constant τ_m shape dendritic filtering
- Explain the compartmental modeling framework and Rall's equivalent cylinder condition
- Describe how active dendritic conductances (Na^+, Ca^{2+}, HCN) transform dendrites from passive cables to computational subunits [5, 6, 8]
- Write down the Tsodyks-Markram model for short-term synaptic plasticity and explain the functional consequences of depression vs. facilitation [17–19]
- Distinguish feedforward from feedback inhibition and explain the inhibition-stabilized network regime [30, 31, 32]
- Compare Izhikevich, AdEx, GIF, and GLIF point-neuron models: equations, parameter counts, and target applications [36–39]
- Evaluate the Rössert et al. BBP simplification pipeline: what network properties survive the collapse to point neurons and what is lost [35]
- Articulate the two-scale modeling requirement for DBS: spatial models for activation, simplified models for network dynamics [52, 55]

Recommended Reading

- London, M. & Häusser, M. (2005). Dendritic computation. *Annu. Rev. Neurosci.* 28:503–532 [5]
- Markram, H. et al. (2015). Reconstruction and simulation of neocortical microcircuitry. *Cell* 163:456–492 [11]
- Rössert, C et al. (2017). Automated point-neuron simplification of data-driven microcircuit models. arXiv:1604.00087v2 [35]
- Brunel, N. (2000). Dynamics of sparsely connected networks of excitatory and inhibitory spiking neurons. *J. Comput. Neurosci.* 8:183–208 [33]
- McIntyre, C.C. et al. (2004). Cellular effects of deep brain stimulation: model-based analysis of activation and inhibition. *J. Neurophysiol.* 91:1457–1469 [52]

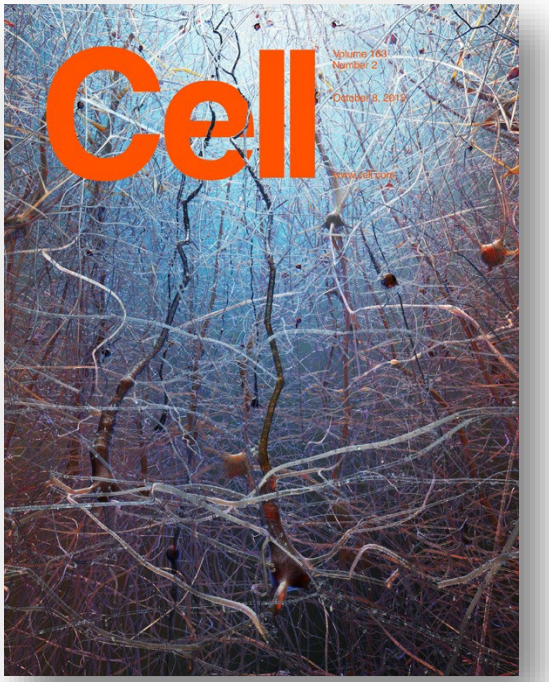

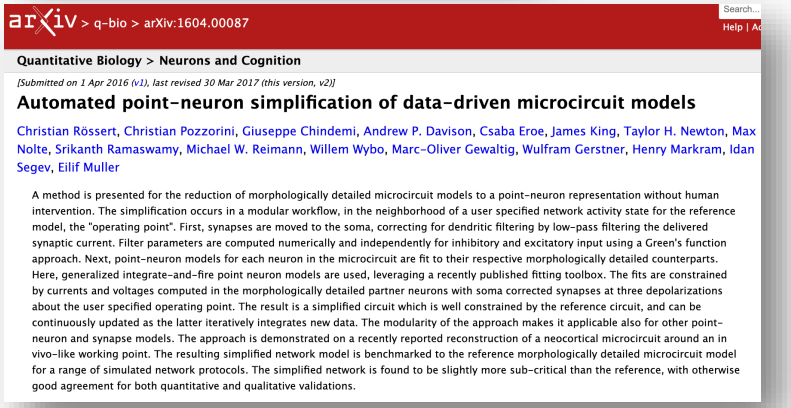
arXiv > q-bio > arXiv:1604.00087

Quantitative Biology > Neurons and Cognition

[Submitted on 1 Apr 2016 (v1), last revised 30 Mar 2017 (this version, v2)]

Automated point-neuron simplification of data-driven microcircuit models

Christian Rössert, Christian Pozzorini, Giuseppe Chindemi, Andrew P. Davison, Csaba Eroe, James King, Taylor H. Newton, Max Nolte, Srikanth Ramaswamy, Michael W. Reimann, Willem Wybo, Marc-Oliver Gewaltig, Wulfram Gerstner, Henry Markram, Idan Segev, Eilif Muller

A method is presented for the reduction of morphologically detailed microcircuit models to a point-neuron representation without human intervention. The simplification occurs in a modular workflow, in the neighborhood of a user specified network activity state for the reference model, the "operating point". First, synapses are moved to the soma, correcting for dendritic filtering by low-pass filtering the delivered synaptic current. Filter parameters are computed numerically and independently for inhibitory and excitatory input using a Green's function approach. Next, point-neuron models for each neuron in the microcircuit are fit to their respective morphologically detailed counterparts. Here, generalized integrate-and-fire point neuron models are used, leveraging a recently published fitting toolbox. The fits are constrained by currents and voltages computed in the morphologically detailed partner neurons with soma corrected synapses at three depolarizations about the user specified operating point. The result is a simplified circuit which is well constrained by the reference circuit, and can be continuously updated as the latter iteratively integrates new data. The modularity of the approach makes it applicable also for other point-neuron and synapse models. The approach is demonstrated on a recently reported reconstruction of a neocortical microcircuit around an in vivo-like working point. The resulting simplified network model is benchmarked to the reference morphologically detailed microcircuit model for a range of simulated network protocols. The simplified network is found to be slightly more sub-critical than the reference, with otherwise good agreement for both quantitative and qualitative validations.

Outline for Today

- **Dendritic Computation — Cable equation, compartmental models, active dendrites**
- Synaptic Mechanisms — TM model, receptor kinetics, E/I balance
- Microcircuit Motifs — Canonical circuits, FFI/FBI, Brunel's phase diagram
- The Simplification Question — Point neuron zoo, BBP pipeline case study
- DBS Circuit Motifs — Two-scale modeling, basal ganglia networks, adaptive DBS
- Exercise Preview — Mini project work

Cable Equation: Geometry Matters

- For a passive cylindrical membrane segment with axial resistance r_a, membrane resistance r_m, membrane capacitance c_m:
$$\lambda^2 \frac{\partial^2 V}{\partial x^2} = \tau_m \frac{\partial V}{\partial t} + V$$
- **Length constant (unmyelinated):** $\lambda = \sqrt{(r_m/r_a)}$ — spatial scale of voltage spread
  - $\lambda \propto \sqrt{d}$ (fiber diameter) — thicker dendrites transmit signals farther
  - $\lambda \propto d$ (approx.) for myelinated internodes
- **Time constant:** $\tau_m = r_m \cdot c_m$ — temporal filtering speed (~10–30 ms, cortical neurons)
- **Electrotonic distance** $L = d_{\text{path}}/\lambda$: the key dimensionless quantity
  - Steady-state attenuation ≈ $\exp(-L)$
  - Typical L5 pyramidal: apical tuft is L ≈ 2–4 from soma → EPSP attenuated to ~2–18%
- Same cable equation as Week 3 (axons) and Week 4 (1D Maxwell reduction) — now applied to dendrites

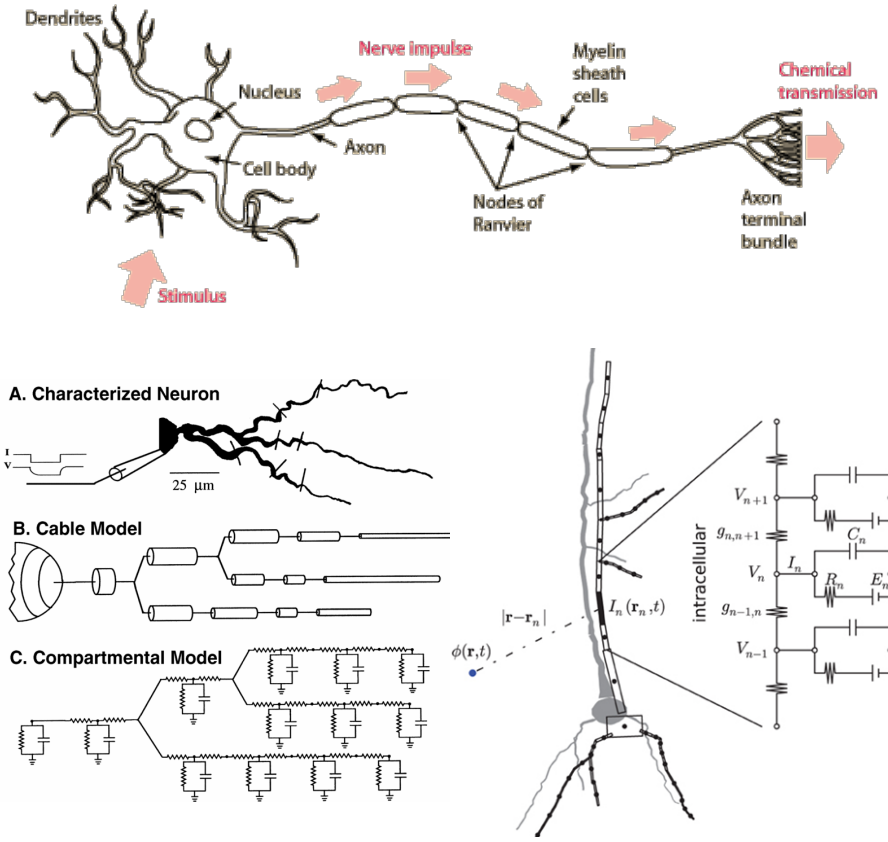

Images: [1–4]

Compartmental Cable Discretization

- Divide the neuron into N isopotential compartments connected by axial conductances [3, 4]

$$C_i \frac{dV_i}{dt} = -g_{L,i}(V_i - E_L) - \sum_j g_{a,ij}(V_i - V_j) + I_{\text{syn},i} + I_{\text{ion},i}(V_i, t)$$

  - Leak | Axial coupling | Synaptic input | Active ion channels
- Each compartment can host **arbitrary nonlinear conductances** (HH, Ca^{2+}, HCN, ...) — unlike analytical cable theory, which requires passive/linear membranes
- **Rall's equivalent cylinder condition** [2]: branching tree collapses to single cylinder if at every branch point:

$$\sum_{\text{daughters (j)}} d_j^{3/2} = d_{\text{parent}}^{3/2}$$

  - Enables analytical solutions for passive branched trees — but real neurons violate it in morphology and in having active channels
- This is the framework used by NEURON (W1), Sim4Life T-NEURO (W6), and all modern compartmental simulators

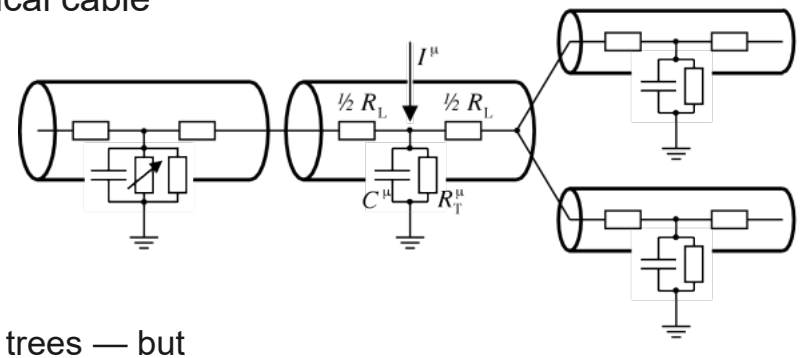

Image: [5]

Active Dendrites (Beyond Passive Cables)

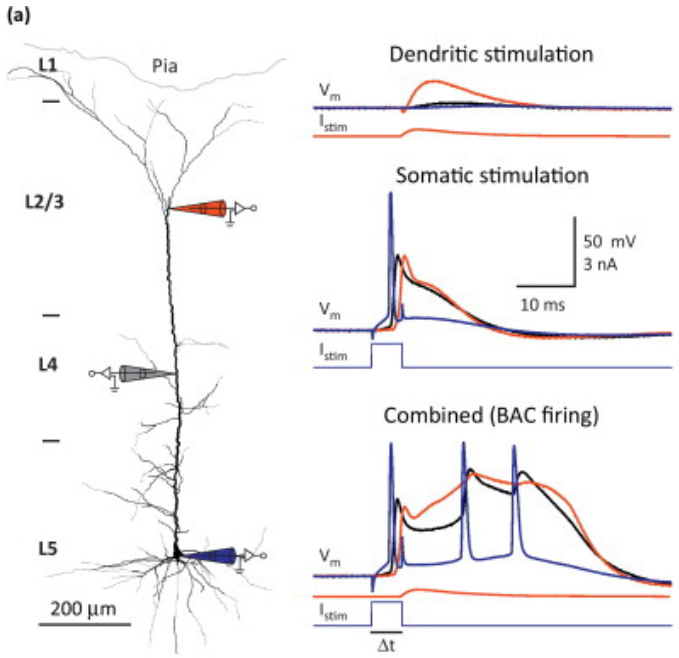

Image: [6]

- **Voltage-gated Na^+ channels** in dendrites → **backpropagating action potentials (bAPs)**
  - Somatic spikes travel retrogradely into the dendritic tree
  - Provide a "somatic output report" to dendritic synapses → basis for Hebbian *spike-time dependent plasticity* (STDP)
- **Voltage-gated Ca^{2+} channels** (L-type, T-type) in apical tuft → **dendritic calcium spikes** [12]
  - Slow plateau potentials (tens of ms, >40 mV amplitude)
  - Overcome passive electrotonic barrier: distal input → Ca^{2+} spike → large somatic depolarization
  - Threshold-dependent: requires sufficient coincident distal input
- **HCN channels (I_h):** hyperpolarization-activated cation current
  - Reduce local input resistance → narrow *excitatory post-synaptic potential* (EPSP) time course in distal dendrites
  - Distance-dependent temporal normalization at the cost of amplitude
- Net effect: the dendritic tree is a **multi-zone computational device** with distinct nonlinear operating regimes, not a passive attenuator [5, 9]

Single Neurons as Two-Layer Networks

- **Poirazi, Brannon & Mel (2003)** [6, 7]: detailed compartmental model of CA1 pyramidal neuron
- **Layer 1 — dendritic branches:** each branch computes a thresholded, saturating function of local synaptic inputs (driven by NMDA voltage dependence + local dendritic spikes)
- **Layer 2 — soma:** ~linear summation of branch outputs → spike generation
- Single neuron with *N* nonlinear branches can solve classification problems a perceptron* cannot — including XOR
- **Key implication:** collapse the neuron to a single compartment and the branch-specific nonlinearity vanishes — see part IV

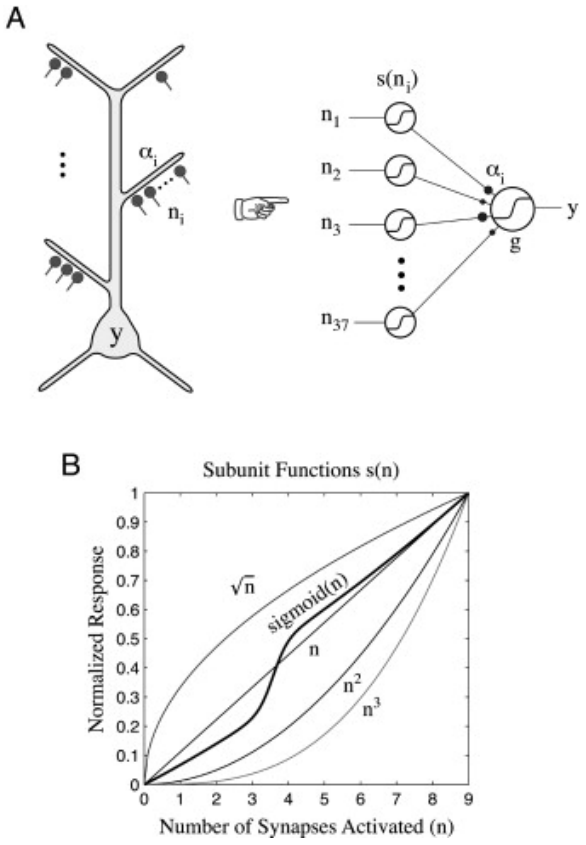

Image: [7]

*Perceptron: computes a weighted sum of its inputs followed by a threshold — equivalent to a linear classifier. It cannot solve problems where classes not linearly separable (e.g., XOR).

BBP and Allen Brain Institute

- **Blue Brain Project** (Markram et al., *Cell* 2015) [11] — recall from W1
  - ~31,000 neurons; 55 morphological types (m-types), 11 electrical types (e-types), 207 morpho-electrical types (me-types); ~8M connections, ~37M synapses
  - Multi-compartment models with realistic morphology, ion channel distributions, algorithmically placed synapses
  - Morphological classification via topological methods (Kanari et al. [16]); NeuroMorpho.Org [15] — largest public repository of digital neuronal reconstructions
- **Allen Institute Cell Types Database** [13, 14]
  - Multimodal characterization: electrophysiology + morphology + transcriptomics
  - Provides generalized leaky integrate-and-fire (**GLIF**) (point) and **all-active** (biophysically detailed) models for many systematically characterized cell classes

*These resources make the **quantitative comparison** between detailed and simplified models possible — what we do in Part IV*

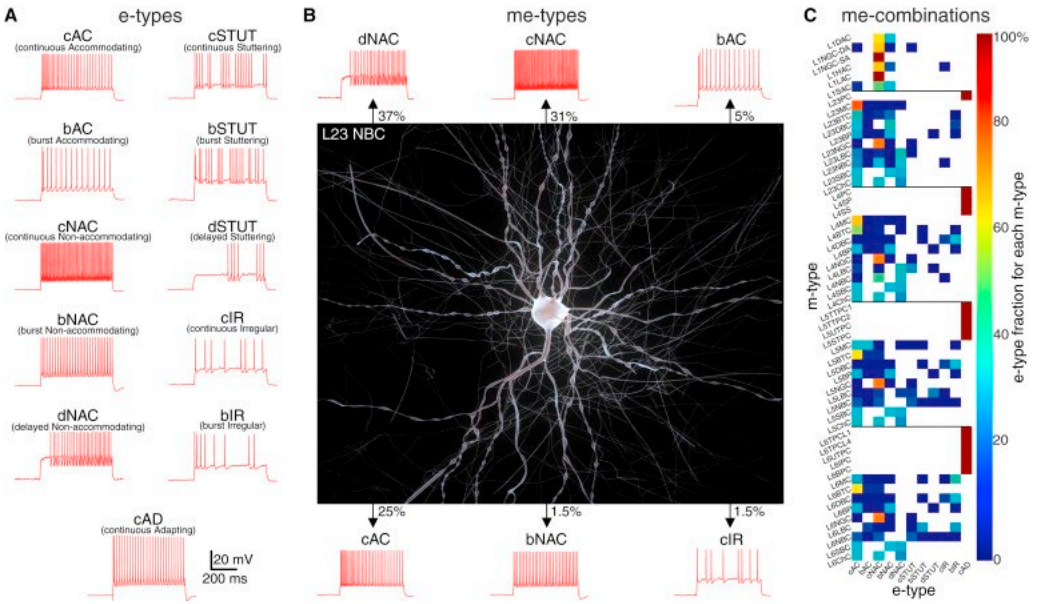

Image: [8]

Outline for Today

- Dendritic Computation — Cable equation, compartmental models, active dendrites
- **Synaptic Mechanisms — TM model, receptor kinetics, E/I balance**
- Microcircuit Motifs — Canonical circuits, FFI/FBI, Brunel's phase diagram
- The Simplification Question — Point neuron zoo, BBP pipeline case study
- DBS Circuit Motifs — Two-scale modeling, basal ganglia networks, adaptive DBS
- Exercise Preview — Mini project work

The Tsodyks-Markram Model

- Synaptic resources in three states: recovered (x), active (y), inactive (z); x + y + z = 1 [17, 19]

$$\frac{dx}{dt} = \frac{z}{\tau_{\mathrm{rec}}} - u \cdot x \cdot \delta(t - t_{\mathrm{sp}}), \quad \frac{dy}{dt} = -\frac{y}{\tau_{\mathrm{in}}} + u \cdot x \cdot \delta(t - t_{\mathrm{sp}})$$

- At each presynaptic spike: fraction u of recovered resources → active state → drives postsynaptic current → inactive state → recovers with τ_{rec}
- **With facilitation**, u itself is dynamic [19]:

$$\frac{du}{dt} = \frac{U - u}{\tau_F} + U(1 - u), \delta(t - t_{\mathrm{sp}})$$

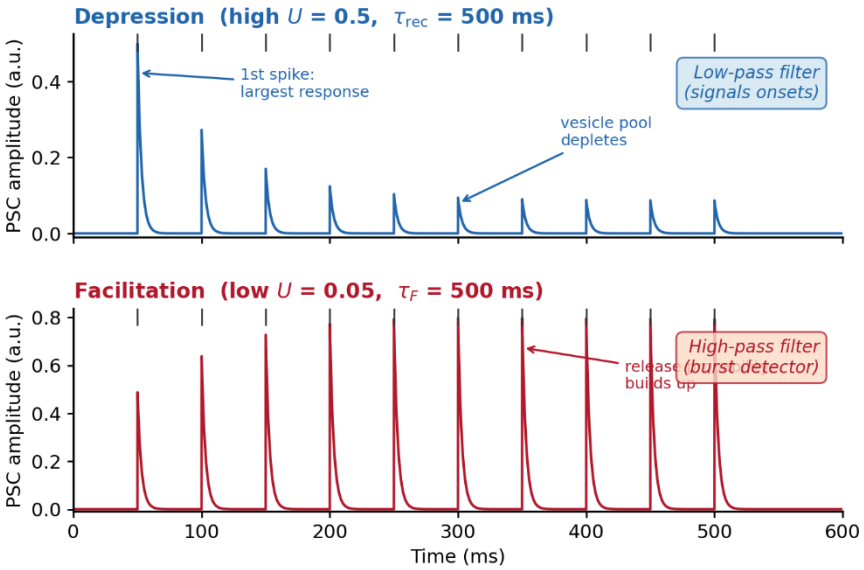

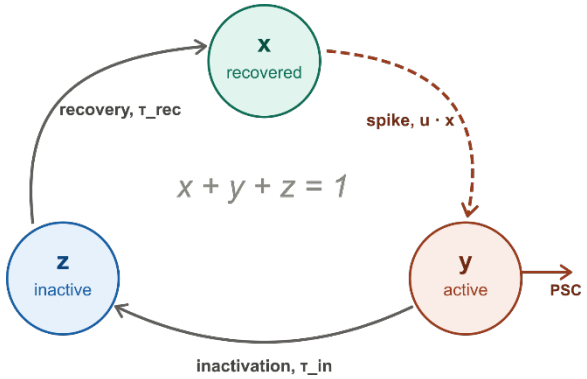

- **High U, fast τ_{rec} → depression:** low-pass filter of PSP amplitude vs. frequency; but preferentially signals onsets after quiescence (first spike = largest response) [21]
- **Low U, large τ_F → facilitation:** high-pass filter / burst detector; transmits single spikes unreliably but responds powerfully to bursts [21]
- **Target-type-specific short-term plasticity** [18]: same presynaptic axon → depressing onto one target class, facilitating onto another → information multiplexing

Channels and Timescales

- General form: $I_R(t) = g_R(t) \cdot (V - E_R)$; $E_{\text{exc}} \approx 0$ mV, $E_{\text{inh}} \approx -75$ mV

Receptor	Type	Rise	Decay	Note
AMPA	EXC, ionotropic	~0.5 ms	2–5 ms	Fast exc drive
NMDA	EXC, ionotropic	~5 ms	50–100 ms	Voltage-dependent Mg2+ block
GABA_A	INH, ionotropic (Cl-)	~1 ms	5–10 ms	Fast inh, spike timing
GABA_B	INH, metabotropic (K+)	~50 ms	100s of ms	Slow, sustained inh

- Kinetic formalism of Destexhe, Mainen & Sejnowski (1994) [24]: unified Markov-state models for all four types — standard in NEURON/Sim4Life
- In the BBP microcircuit [11]: excitatory synapses = AMPA + NMDA; inhibitory = GABA_A + GABA_B; presynaptic dynamics = TM model [17–19]

NMDA and Dendritic Nonlinearities

- NMDA conductance is voltage-dependent due to extracellular Mg^{2+} block [22, 23]:

$$g_{\mathrm{NMDA}}(V) = \overline{g_{\mathrm{NMDA}}} \cdot s(t) \cdot \frac{1}{1 + [\mathrm{Mg}^{2+}]_o \cdot e^{-\gamma V}/\beta}$$

  - At rest (~−70 mV): channel strongly blocked (B(V) ≈ 0.1) → negligible current
  - Block progressively relieved by depolarization; near-maximal conductance by 0 mV
  - Exact shape of B(V) depends on parameterization; qualitative behavior is robust
- **In thin distal dendrites** (high local R_{input}): a few AMPA EPSPs provide enough local depolarization to relieve Mg^{2+} block → subsequent NMDA current flows → **supralinear summation**
- This is the biophysical engine of the Poirazi et al. "two-layer network" [6]: the branch nonlinearity is an NMDA-dependent phenomenon whose expression **requires spatial segregation of inputs on distinct branches**
- **Collapse to a point neuron → this branch-specific nonlinearity vanishes.** All NMDA and AMPA currents sum at a single compartment; no branch can independently reach the Mg^{2+} unblock threshold.

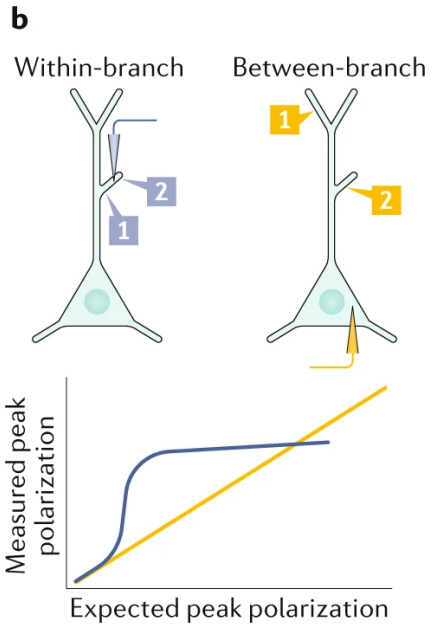

Image: [9]

NMDA and Dendritic Nonlinearities

- NMDA conductance is voltage-dependent due to extracellular Mg^{2+} block [22, 23]:

$$g_{\mathrm{NMDA}}(V) = \overline{g_{\mathrm{NMDA}}} \cdot s(t) \cdot \frac{1}{1 + \frac{[Mg^{2+}]_o}{\beta} e^{-\gamma V}}$$

  - At res… → negli…
  - Block… imal condu…
  - Exact… ative behav…
- **In thin dist…** PSPs provide enc… → subsequent… **on**
- This is the b… r network" [6]… nt phenomenc… **tion of inputs on distinct branches**
- **Collapse to a point neuron → this branch-specific nonlinearity vanishes.** All NMDA and AMPA currents sum at a single compartment; no branch can independently reach the Mg^{2+} unblock threshold.

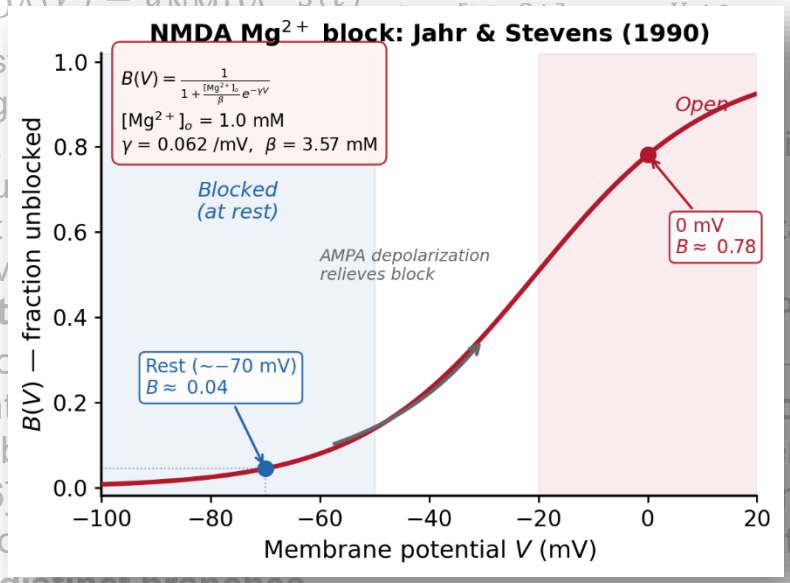

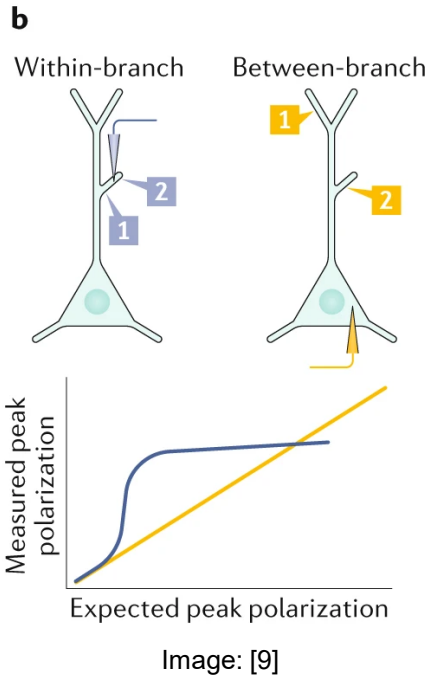

Image: [9]

EXC/INH Balance; Cortical Operating Regime

- Conductance-based membrane equation with excitatory and inhibitory synaptic input:

$$C_m \frac{dV}{dt} = -g_L(V - E_L) - g_E(t)(V - E_E) - g_I(t)(V - E_I)$$

- In the **balanced regime**: mean net synaptic current ≈ 0 → mean V sits below threshold → **spiking is driven by fluctuations** in the balance, not by net excitation
- Experimentally confirmed:
  - **Shu, Hasenstaub & McCormick (2003)** [25]: excitatory and inhibitory conductances co-activate during UP states in ferret cortex *in vivo*
  - **Okun & Lampl (2008)** [26]: instantaneous (moment-by-moment) E/I correlation during spontaneous and evoked activity
- **Denève & Machens (2016)** [27]: tight E/I balance can implement efficient predictive coding — inhibition cancels predicted excitation; only prediction error drives spikes
- **For the simplification question:** E/I balance is a macroscopic network property. It **does not require morphological detail** to maintain — point neurons with appropriate E/I input reproduce the fluctuation-driven regime. This is one reason simplification works.

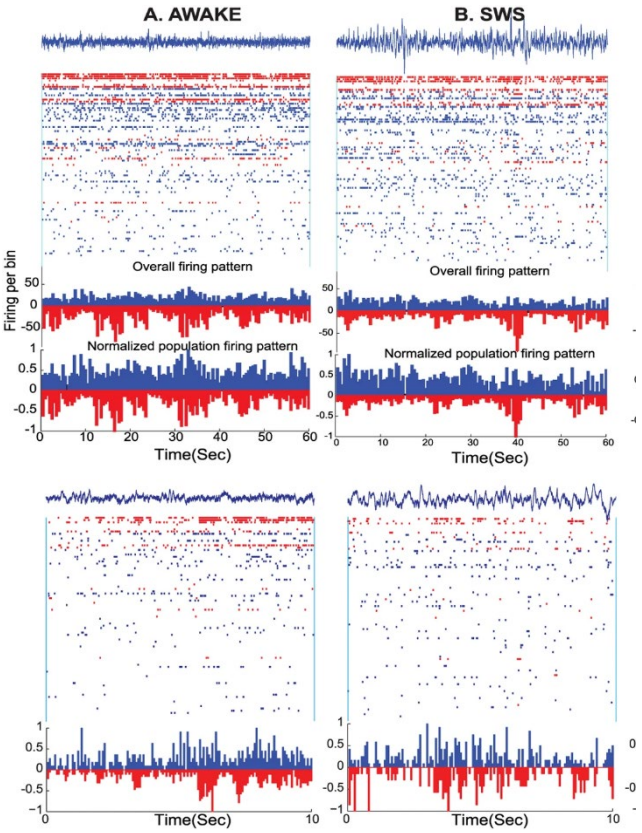

Image: [10]

Outline for Today

- Dendritic Computation — Cable equation, compartmental models, active dendrites
- Synaptic Mechanisms — TM model, receptor kinetics, E/I balance
- **Microcircuit Motifs — Canonical circuits, FFI/FBI, Brunel's phase diagram**
- The Simplification Question — Point neuron zoo, BBP pipeline case study
- DBS Circuit Motifs — Two-scale modeling, basal ganglia networks, adaptive DBS
- Exercise Preview — Mini project work

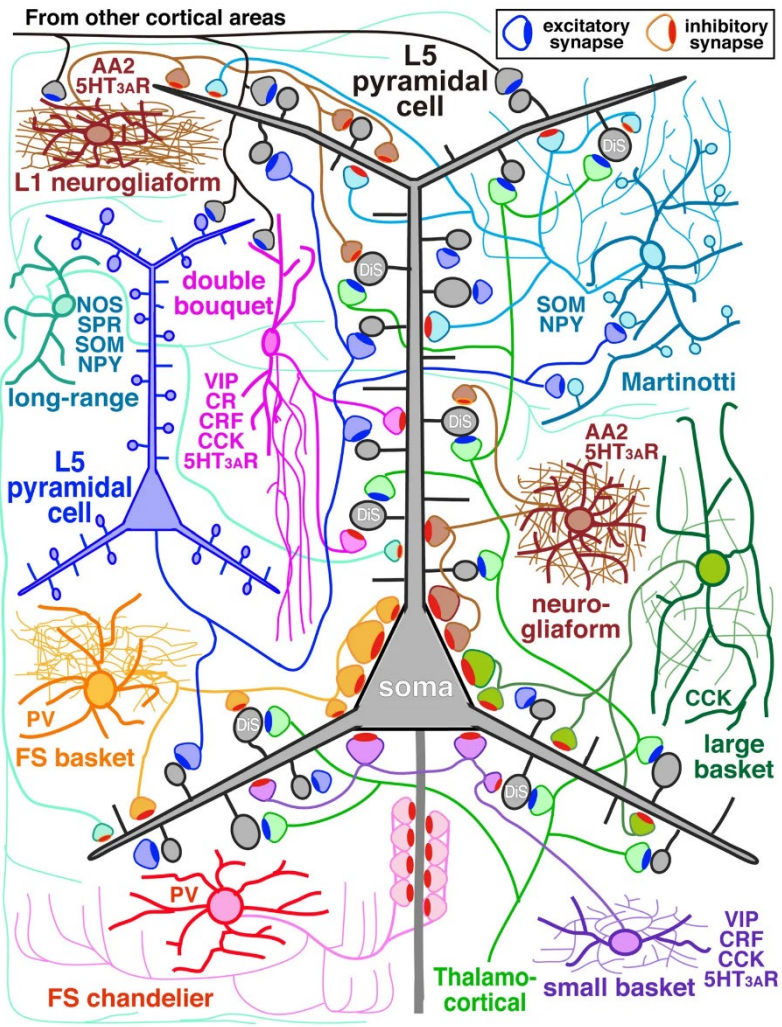

Image: [11]

The "Cortical Column"

- **Douglas & Martin (1991, 2004)** [28, 29]: a recurring circuit template across cortical areas
  - Excitatory pyramidal neurons (L2/3, L4, L5)
  - Inhibitory interneurons (basket cells, Martinotti cells, ...)
  - Thalamocortical input → L4
  - Basic computational "unit" for the cortex
- Key insight: **recurrent intracortical excitation >> feedforward thalamic drive**
  - Subsequent anatomical studies in sensory cortex confirmed thalamic input provides only a small fraction (~5–10%) of excitatory synapses onto L4 neurons
  - Intracortical amplifier boosts this weak signal substantially through recurrent excitation
  - Inhibition prevents runaway → **recurrent amplifier with inhibitory stabilization**
- **Implication for stimulation:** when an electrode activates cortical neurons, the recurrent amplifier determines how activation propagates — not just the direct E-field footprint

Feedforward vs. Feedback Inhibition

- **Feedforward inhibition (FFI)** [30]:
  - Excitatory input activates both principal cells AND local interneurons
  - Interneurons fire first (lower threshold, faster τ_m) → disynaptic IPSP arrives within 1–3 ms
  - Creates narrow **temporal window** (~5 ms) for spike generation
  - Enforces temporal fidelity + gain normalization
- **Feedback inhibition (FBI) — Martinotti cell motif** [31]:
  - Pyramidal cell output → Martinotti cell (via **facilitating** synapse) → inhibition back onto pyramidal cell **apical dendrites**
  - Frequency-dependent: weak during sparse firing, strong during bursts
  - **Targets dendrites, not soma** — controls dendritic integration, not spike output
- **Point-neuron consequence:** FFI and FBI, perisomatic (basket cell) and dendritic (Martinotti) inhibition all collapse to a single inhibitory input → loss of compartment-specific control

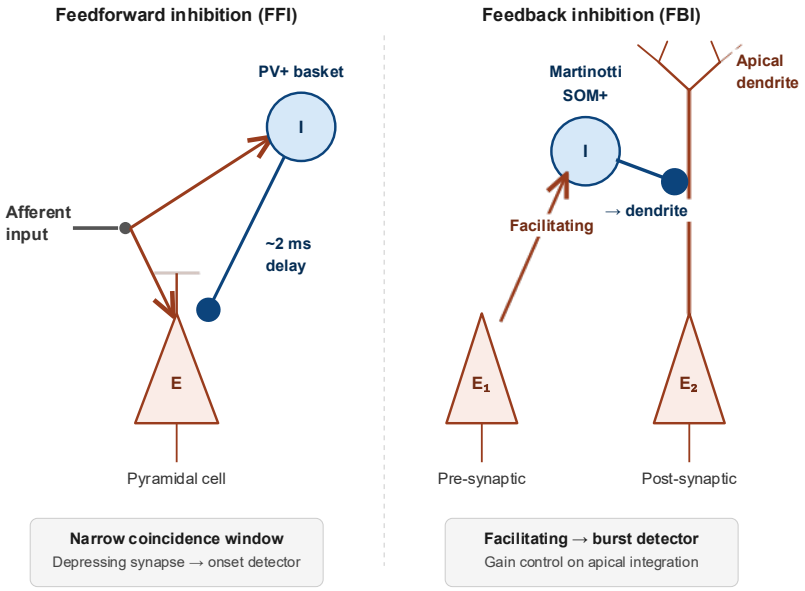

Inhibition-Stabilized Networks (ISN)

Two-population rate model [32, 34]:

$$\tau_I \frac{dr_I}{dt} = -r_I + f(W_{IE}, r_E - W_{II}, r_I + h_I) \tau_E \frac{dr_E}{dt} = -r_E + f(W_{EE}, r_E - W_{EI}, r_I + h_E)$$

- **ISN regime:** recurrent excitation W_EE strong enough that E population is unstable alone — stability maintained only by feedback inhibition from I
- **Hallmark — "paradoxical" response:** directly injecting excitatory current into I population can *decrease* I steady-state firing rate — because the initial increase in inhibition suppresses E neurons, which withdraws the recurrent drive to I
- **Ozeki et al. (2009)** [32]: ISN regime explains visual surround suppression — expanding stimulus causes withdrawal of both E and I drive, with E reduction dominating → net suppression
- **For neuromodulation:** the ISN regime means stimulation effects cannot be predicted from simple feedforward reasoning — activating E neurons recruits compensatory inhibition; circuit response depends on recurrent dynamics

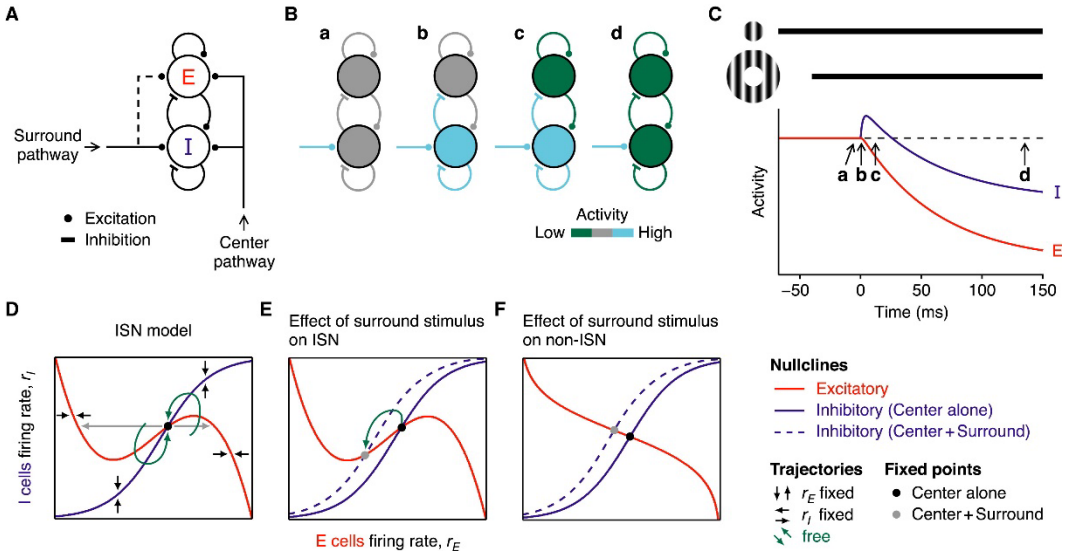

Image: [12]

Point Neuron Network Dynamics

- **Brunel (2000)** [33]: analytical phase diagram for large, sparse networks of LIF neurons
- Key parameters: $g = W_I/W_E$ (inhibition/excitation ratio); ν_{ext} (external drive)

	Low synchrony	High synchrony
Regular	Asynchronous Regular (AR)	Synchronous Regular (SR)
Irregular	Asynchronous Irregular (AI)	Synchronous Irregular (SI)

- **AI state** matches cortical activity *in vivo*: irregular firing, low rates, ~Poisson statistics, weak pairwise correlations
  - Requires inhibition to dominate (g sufficiently large) + sufficient external drive
  - Mean input subthreshold (cancelled by inhibition); spikes from fluctuations
- **Performed entirely with point LIF neurons** — demonstrating that qualitative cortical network dynamics do not require morphological detail
- **But:** assumes homogeneous, uncorrelated input — dendritic processing violates this. When does it matter? → Part IV

Brunel's Phase Diagram

Point Neuron Network Dynamics

- **Brunel (**
  neurons
- Key para

Regular

Irregular

- **AI state**
  statistics
  - Re
  - Me
- **Perform**
  cortical r
- **But:** assumes homogeneous, uncorrelated input — dendritic processing violates this. When does it matter? → Part IV

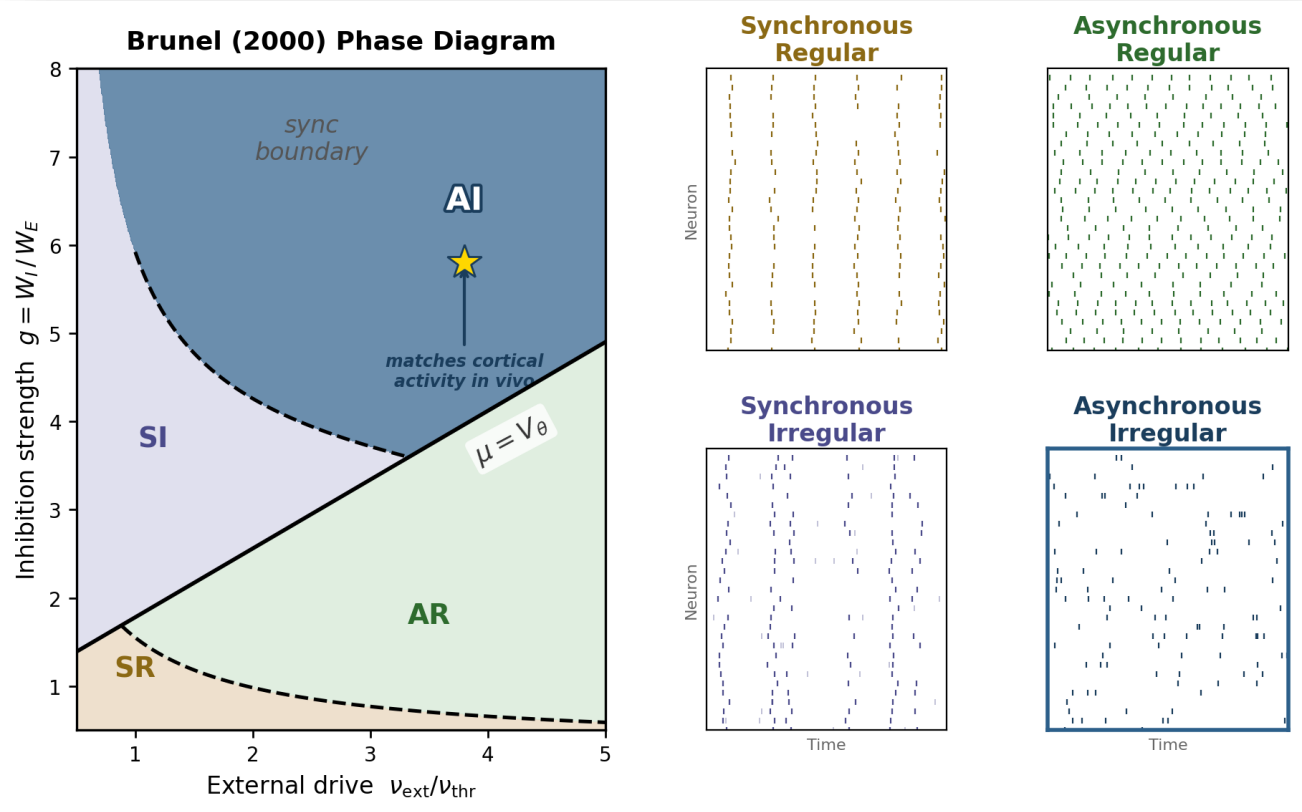

Outline for Today

- Dendritic Computation — Cable equation, compartmental models, active dendrites
- Synaptic Mechanisms — TM model, receptor kinetics, E/I balance
- Microcircuit Motifs — Canonical circuits, FFI/FBI, Brunel's phase diagram
- **The Simplification Question — Point neuron zoo, BBP pipeline case study**
- DBS Circuit Motifs — Two-scale modeling, basal ganglia networks, adaptive DBS
- Exercise Preview — Mini project work

Point Neuron Zoo

- **Leaky Integrate-and-Fire (LIF):** $C_m dV/dt = -g_L(V - E_L) + I_{\text{syn}};$ spike if $V \geq V_{\text{th}}$, reset $V \to V_r$
  - 1 ODE, ~3 floating point operations per sec (FLOPS) / step. Used in Brunel's analysis [33]
- **Izhikevich (2003)** [37]: $dv/dt = 0.04v^2 + 5v + 140 - u + I; du/dt = a(bv - u)$
  - 2 ODEs, 4 parameters (a,b,c,d), ~13 FLOPS / step. >20 firing patterns
- **AdEx** (Brette & Gerstner, 2005) [38]:
  - $C\frac{dV}{dt} = -g_L(V - E_L) + g_L\Delta_T \cdot \mathrm{e}^{\left(\frac{V - V_T}{\Delta_T}\right)} - w + I_{\text{syn}}$
  - $\tau_w \frac{dw}{dt} = a(V - E_L) - w;$ spike reset: $V \to V_r;\ w \to w + b$
  - ~96% spike-time prediction accuracy (within ±2 ms) vs. a detailed HH model under fluctuating conductance injection [38]. Default for large-scale spiking networks
- **GIF** (Pozzorini et al., 2015) [36]:
  - $C\frac{dV}{dt} = -g_L(V - E_L) + I_{\text{syn}} - \eta(t);\quad$ spike if $V \geq V_T(t)$
  - $V_T(t) = V_T^* + \sum_{t_j<t} \gamma(t - t_j)$
  - $\eta(t)$ = spike-triggered current kernel; $\gamma(t)$ = spike-triggered threshold kernel
  - Convex log-likelihood → unique optimum → automated high-throughput fitting
  - Used in BBP simplification pipeline [35]
- **GLIF** (Teeter et al., 2018) [39]: 5-level hierarchy; fitted to Allen Cell Types Database
  - Standardized simplified models for many experimentally characterized cell classes

Image: [3]

Point Neurons: Tradeoffs

Point Neuron Zoo

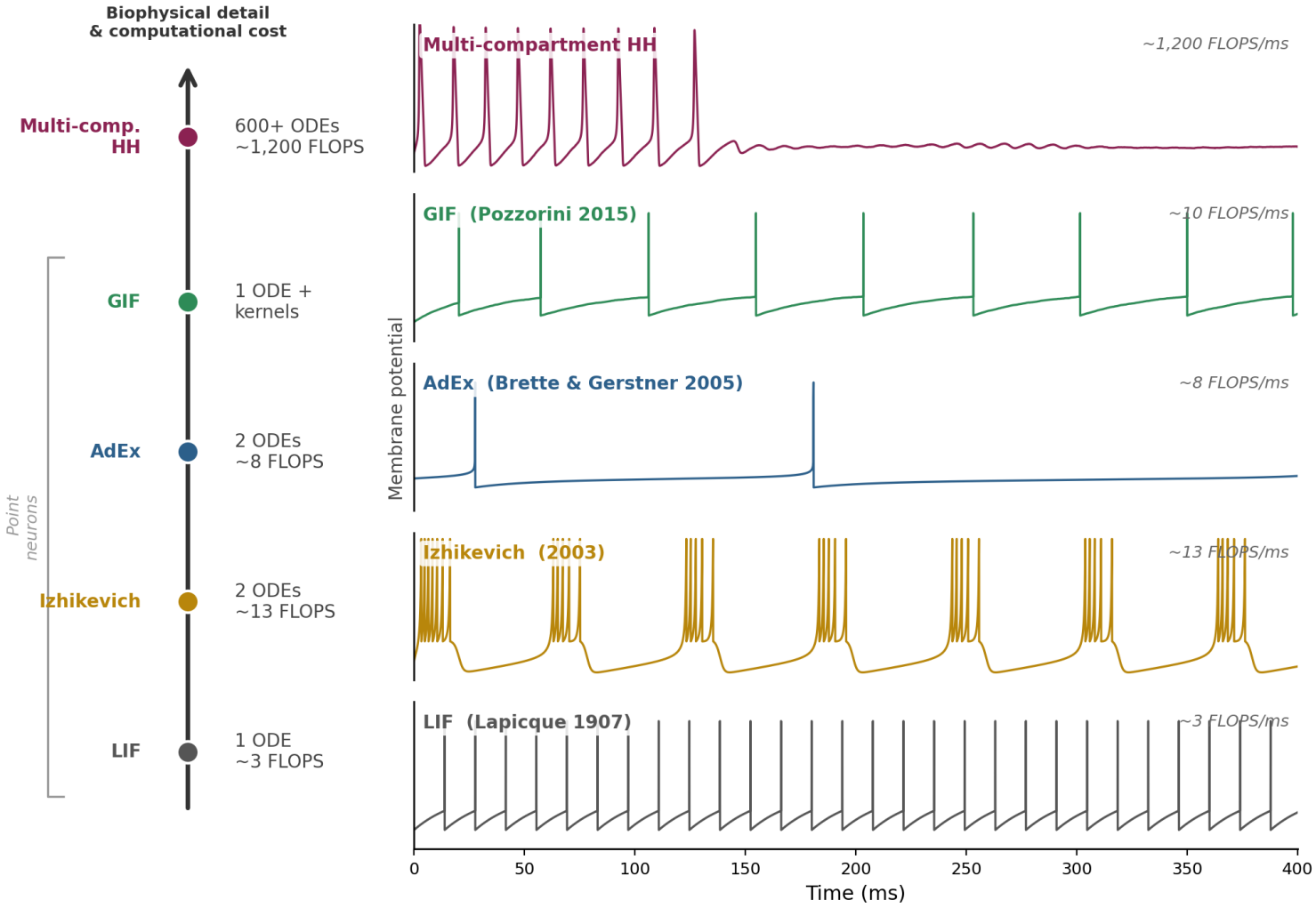

What Is Lost When You Collapse to a Point?

1. **Spatial selectivity of extracellular stimulation**
   - Activating function $f(x) = \partial^2 V\_e/\partial x^2$ (W3) requires spatial extent along neural processes
   - Axon depolarized while soma is hyperpolarized by the same electrode → invisible to a point neuron
2. **Dendritic nonlinearities**
   - NMDA branch-specific supralinear summation, Ca^{2+} dendritic spikes → abolished
   - Neuron becomes a single integrator (perceptron), not a two-layer network
3. **Location-dependent inhibition**
   - Perisomatic (basket cell) vs. dendritic (Martinotti) inhibition → collapse to one input
4. **Dendritic filtering of synaptic input**
   - Distal EPSP: attenuated, broadened; proximal EPSP: fast, large → all identical at a point
5. **Backpropagation-dependent plasticity**
   - STDP requiring bAP at dendritic synapse sites → no spatial dimension to propagate through

Gains: 1–3 orders of magnitude in computational cost; analytical tractability (cf. Brunel [33])

Image: [3]

Point Neuron Collapse

What Is Lost When You Collapse to a Point?

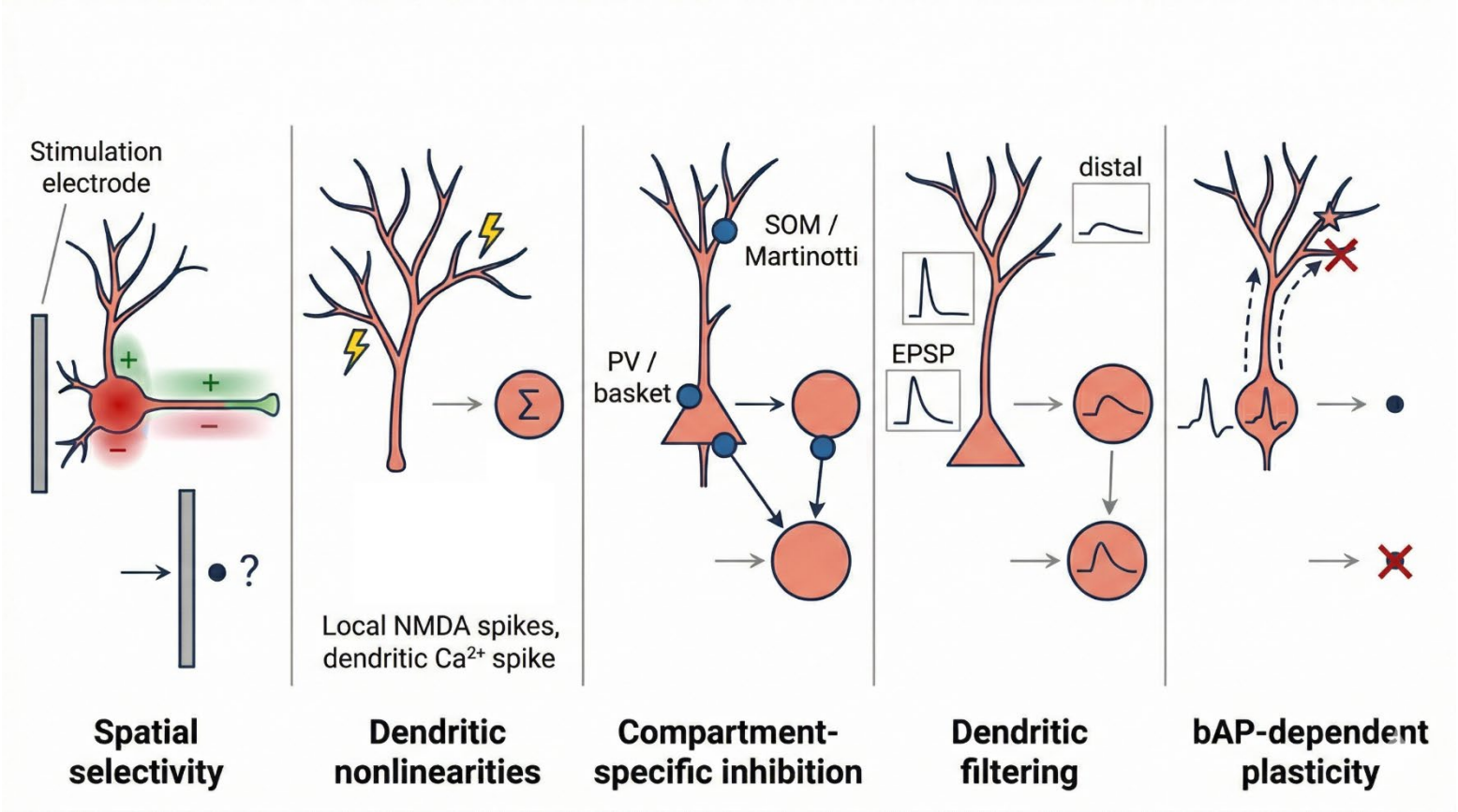

Automated Point-Neuron Simplification of a Data-Driven Microcircuit

- **Rössert et al. (2017)** [35]: reduce the full BBP microcircuit (~31,000 neurons, ~37M synapses [11]) to GIF point neurons [36] — without human intervention
- **Two-step modular pipeline**, constrained at the *in vivo*-like operating point:
- **Step 1 — Soma-synaptic correction:**
  - Move all synapses to soma, but equip each with a corrective low-pass filter preserving the somatic EPSP
- **Step 2 — Neuron simplification:**
  - Replace each detailed neuron with a GIF model fit to its individual somatic response
- **Operating point principle:** simplification is optimized for a specific network state (100% rheobase, $\left[Ca^{2+}\right]_o$ = 1.25 mM). Validity degrades as the network moves away from this state.
- Pipeline is automated and modular → continuously re-derivable as reference model integrates new data

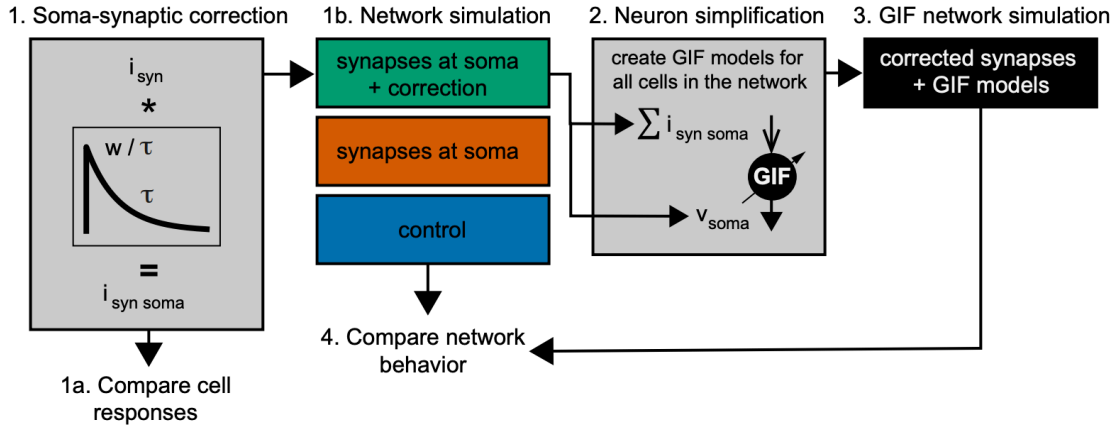

Image: [13]

Figure 1: Automated point-neuron simplification procedure. The procedure of automated point-neuron simplification can be separated into two main parts: 1. soma-synaptic correction and 2. neuron simplification.

Step 1: Soma-Synaptic Correction via Green's Functions

- **Problem:** moving a synapse from dendrite to soma changes the somatic EPSP waveform
- **Solution:** each synapse gets a corrective low-pass filter:
  $\tau \frac{d}{dt}, i_{\text{syn,soma}} = -i_{\text{syn,soma}} + w \cdot i_{\text{syn}}$
- **Intuition:** dendrite acts as a low-pass filter from synapse → soma (smooths and delays). The Green's function is its impulse response. Moving the synapse to the soma removes this filter, κ(ω) puts it back.
- Filter kernel κ(ω) [35]:
  $\kappa(\omega) = \widetilde{V^D}(\omega)/\widetilde{V^S}(\omega)$
  - V^D = somatic PSP with synapse on dendrite; V^S = somatic PSP with synapse at soma

Image: [13]

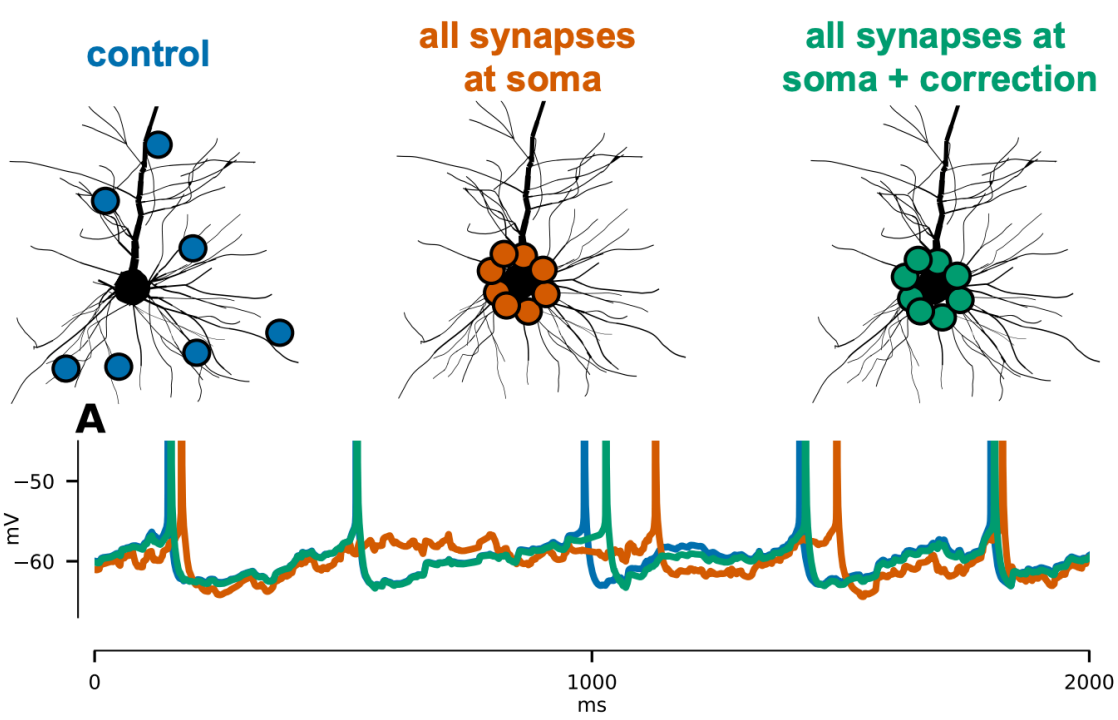

- **Key findings for L5 TTPC:**
  - τ: ~0 ms (proximal) → ~35 ms (distal apical tuft)
  - w: ~1.0 (proximal) → <0.1 (distal) — >90% attenuation
  - Inhibitory synapses need separate filters
  - Full per-compartment diversity reducible to **k = 3–5 clusters**

Step 2: GIF Model Fitting and Network-Level Validation

- Each neuron replaced by a *generalized integrate-and-fire* (**GIF**) **model** [36] fit to individual somatic response at 3 depolarization levels (93%, 100%, 120% rheobase)
  - 14 free parameters per model (C, g_L, E_L,V_T^*, V_{reset}, ΔV, η(t), γ(t) kernels)
  - Successful fits for ~80% of neurons; remainder replaced by same "morpho-electrical"-type GIF
- **What the simplified network preserves:**
  - PSP amplitude matrix across 1,941 pathways (55 × 55 m-types): qualitatively preserved
  - Critical $\left[Ca^{2+}\right]_o$ for asynchronous → synchronous transition: preserved
  - Sensory-evoked PSTHs: high linear correlation with reference; ON/OFF/NR cell identity maintained
  - Response variability: comparable trial-to-trial SD of first-spike latency

Image: [13]

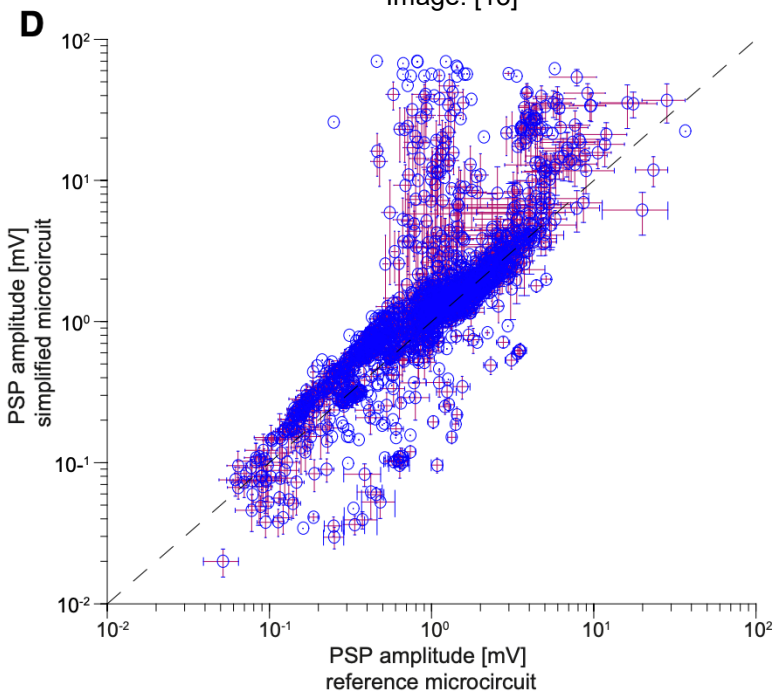

Point Neuron Collapse: Quantitative Deficits

- **Spatial correlations halved:** correlated activity between nearby neuron clusters decays faster (τ_space ≈ 176 µm vs. 284 µm in reference) — the clearest signature that dendrites shape spatial structure
- **Weaker response propagation:** central stimulus responses preserved at ~75%, but spread to distant neurons is markedly reduced
- **Sub-criticality shift:** simplified network sits further from the edge of synchrony; subtle but affects all of the above
- **Operating point caveat:** these deficits are measured near the calibrated baseline: *stimulation perturbs the network away from it*, potentially making the approximation worse

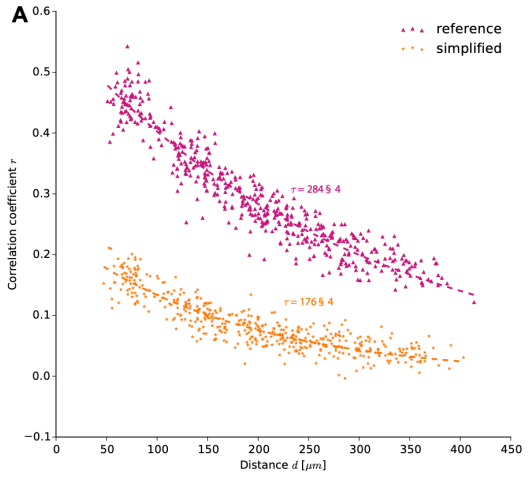

Image: [13]

From CPUs to Neuromorphic Chips

- **CPU-based simulators** (recall from W1):
  - **NEST** [42]: MPI/thread parallelism; standard for >10^6 point neurons
  - **Brian 2** [44]: equation-centric Python API; code generation for C++/GPU
  - **CoreNEURON** [47]: GPU engine for NEURON — brings detailed models to point-neuron scale
  - **PyNN** [46]: simulator-independent API across NEURON, NEST, Brian
- **GPU-accelerated:**
  - **GeNN** [45]: up to 200× speedup for 10^6-neuron HH networks
- **Neuromorphic hardware** (real-time / ultra-low-power):
  - **SpiNNaker** [48]: many ARM cores, real-time simulation at extreme scale
  - **Intel Loihi** [49]: 128 neuromorphic cores, on-chip spike time-dependent plasticity
  - **BrainScaleS-2** [50, 51]: analog neurons, 1,000× biological real-time
- Neuromorphic platforms **require** point-neuron models → the detailed-to-simplified pipeline is essential for translating biophysically grounded models to hardware deployment

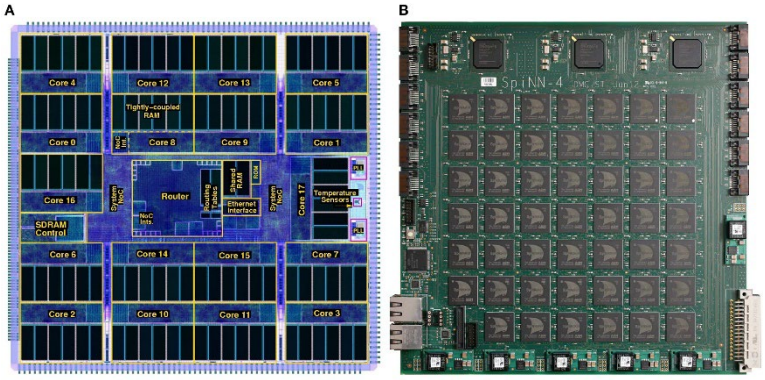

The SpiNNaker chip

A 48-node SpiNNaker board (SpiNN-4)

Image: [14]

Outline for Today

- Dendritic Computation — Cable equation, compartmental models, active dendrites
- Synaptic Mechanisms — TM model, receptor kinetics, E/I balance
- Microcircuit Motifs — Canonical circuits, FFI/FBI, Brunel's phase diagram
- The Simplification Question — Point neuron zoo, BBP pipeline case study
- **DBS Circuit Motifs — Two-scale modeling, basal ganglia networks, adaptive DBS**
- Exercise Preview — Mini project work

DBS: Abstractions With Clinical Consequences

- **Scale 1 — Which neural elements are activated?** (spatial question)
  - Activating function $f(x) = \partial^2 V_e / \partial x^2$ computed from extracellular field [64, 65], assumes fiber orientation
  - Hessian approach [70]: $H_{ij} = \partial^2 V_e / \partial x_i \partial x_j$ largest eigenvalue gives maximum AF over all orientations at each point → orientation-independent volume of tissue activated (VTA) without tracing fibers
  - Full threshold titration (does this neuron fire?) still requires multi-compartment cable models [55]
  - *Point neurons cannot answer this question* — no axon/soma distinction
- **Scale 2 — How does the network respond?** (dynamic question)
  - Circuit-level consequences: oscillation suppression, information flow restoration
  - Captured by simplified conductance-based or point-neuron models
- **McIntyre et al. (2004)** [52]: DBS simultaneously **activates efferent axons** AND **suppresses somatic firing**
  - Axonal activation → drive at stimulus frequency to downstream targets
  - Somatic suppression — consistent with depolarization block and sodium-channel inactivation
  - Resolves the DBS paradox: "lesion-like" locally, excitation in projections
  - **Impossible to obtain with point neurons** — requires resolving the axon/soma spatial relationship

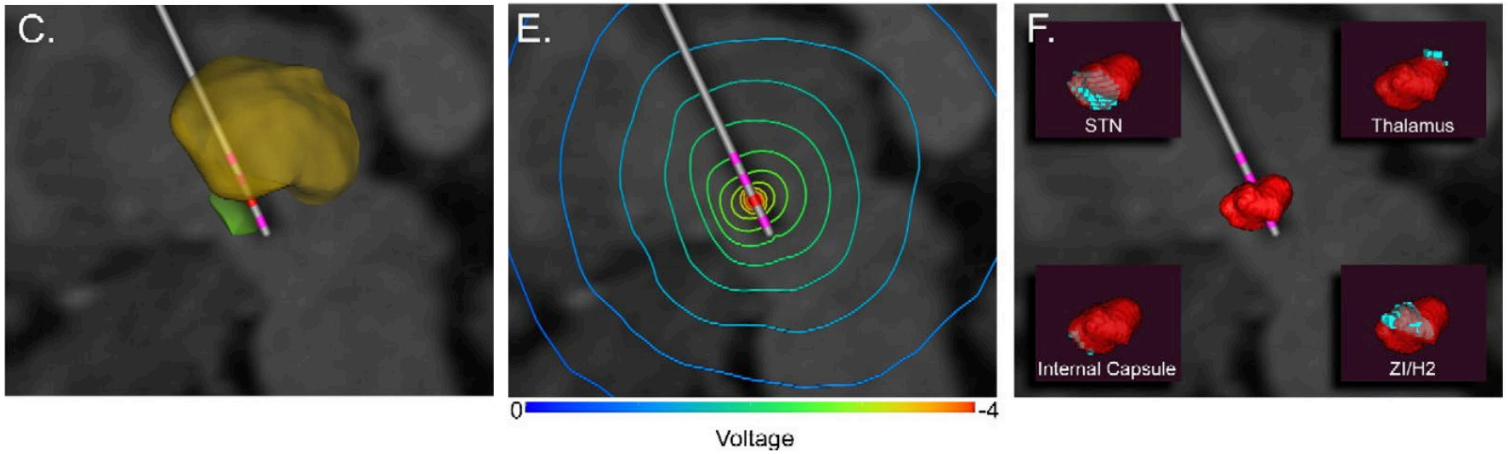

Image: [15]

Basal Ganglia Network Models

- **Rubin & Terman (2004)** [56]: STN-GPe-GPi loop model
  - HF-DBS of STN → regularizes GPi firing (tonic, non-bursty) → thalamus can relay cortical signals
  - Parkinsonian state: GPi bursting/pausing → disrupted thalamic relay
  - Used simplified conductance-based neurons — **no dendritic morphology needed**
- **Grill, Snyder & Miocinovic (2004)** [54]: **informational lesion** hypothesis
  - DBS overwrites pathological oscillatory/bursty patterns with regular HF firing on projection axons

- **Kumaravelu, Brocker & Grill (2016)** [58]: full cortex-basal ganglia-thalamus model
  - Tested closed-loop strategies: stimulation optimized for firing regularity outperforms conventional high frequency-DBS
- **Lead-DBS** [61]: clinical toolbox integrating electrode localization + VTA + connectivity analysis
- Common theme: **spatial models for activation** (Scale 1) + **network models for dynamics** (Scale 2)

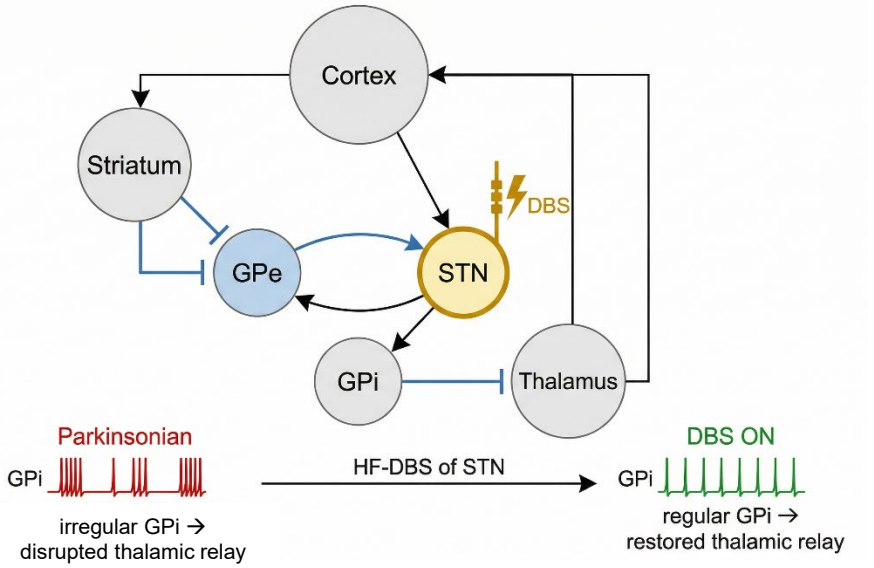

Image: [16]

Basal Ganglia Network Anatomy

Kiani et al., *Sci Rep*, 2023 (Fig 2): Basal ganglia regions with direct and indirect pathways. STR: Striatum, GPe: Globus Pallidus external, GPi Globus Pallidus internal, STN: SubThalamic Nucleus, Th: Thalamus, HC: Hippocampus, VTA: Ventral Tegmental Area, SNc: Substantia Nigra pars compacta, SNr: Substantia Nigra pars reticular, DS: Dorsal Striatum (including Putamen and Caudate), VS: Ventral Striatum (Nucleus Accumbens (NAc) and Olfactory Tubercle (OT)), D1: Excitatory dopamine receptors, D2: Inhibitory dopamine receptors.

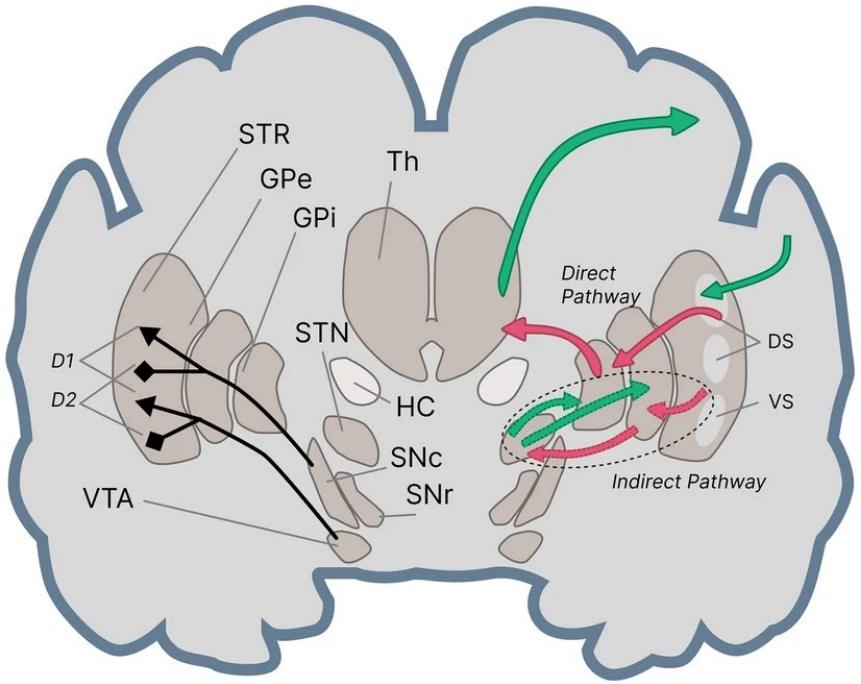

Image: [17]

Adaptive DBS

- **Closed-loop DBS** adjusts stimulation based on real-time neural biomarkers
  - Biomarker (beta-band LFP power) = **network-level signal** → captured by simplified models
  - Stimulation effect = **VTA + activation pattern** → requires spatial models
- **Fleming, Dunn & Lowery (2020)** [62]: simulated closed-loop suppression of pathological beta oscillations using PI control of a cortex-basal ganglia-thalamus network model
- **Fleming et al. (2021)** [63]: multi-contact directional leads with independently controlled contacts → improved efficacy and battery life

- **Clinical embodiment:** Medtronic announced FDA approval for **BrainSense Adaptive DBS** in Feb 2025 [69]
  - >40,000 patients worldwide have Percept devices
- **Full adaptive DBS pipeline:** multi-compartment models for activation prediction, point-neuron networks for dynamics, and control theory for feedback optimization

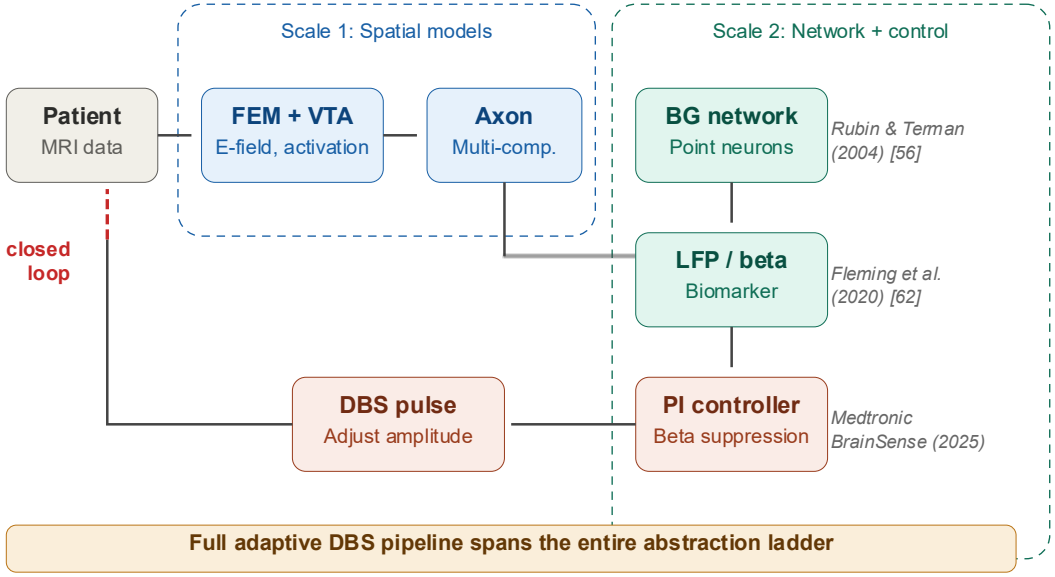

Key Takeaways

1. **Dendritic morphology matters** when the question involves spatial selectivity of extracellular fields (activating function, VTA), dendritic nonlinearities (NMDA-dependent branch computation, Ca^{2+} spikes), or compartment-specific inhibition

2. **Synaptic mechanisms are the bridge** — STP (TM model), receptor kinetics, and E/I balance determine how activation propagates through circuits; these can be preserved in simplified models but require explicit correction for dendritic filtering (soma-synaptic correction)

3. **Network-level dynamics can often be captured by point neurons** provided E/I balance and connectivity structure are preserved — Rössert et al. [35]: sensory responses and state transitions survive; spatial correlations (τ halved) and near-critical temporal structure do not

4. **DBS exemplifies the multi-scale requirement** — VTA requires spatial models (Scale 1); circuit dynamics use simplified models (Scale 2); adaptive DBS requires both simultaneously

5. **Abstraction level is a design choice, not a hierarchy of quality** — match the model to the question

Outline for Today

- Dendritic Computation — Cable equation, compartmental models, active dendrites
- Synaptic Mechanisms — TM model, receptor kinetics, E/I balance
- Microcircuit Motifs — Canonical circuits, FFI/FBI, Brunel's phase diagram
- The Simplification Question — Point neuron zoo, BBP pipeline case study
- DBS Circuit Motifs — Two-scale modeling, basal ganglia networks, adaptive DBS
- **Exercise Preview — Mini project work**

Exercise: Mini Project Work Session

- **This week:** dedicated time for supervised mini project work
- Apply concepts from Weeks 1–7 to your chosen project topic
- Consider the abstraction-level question for your own project:
  - What is the minimum level of biophysical detail your question requires?
  - Where can you simplify without changing the answer?
- Office hours available for project consultation
- **Reminder:** project presentations in Week 13 (28.05.2026)

Image Credits

[1] Hines et al. (2001). Neuroscientist 7(2):123–135
[2] McIntyre et al (2002). J Neurophysiol. 87(2): 995–1006.
[3] Reilly et al. (1985). IEEE Trans Biomed Eng 32(12): 1001–1011
[4] Sweeney et al. (1986) Proceedings of the 9th IEEE Annual Conference of Engineering in Medicine and Biology Society: 1577–1578
[5] W. Gerstner, W. M. Kistler, R. Naud, and L. Paninski, *Neuronal Dynamics: From Single Neurons to Networks and Models of Cognition*. Cambridge, UK: Cambridge University Press, 2014
[6] M. E. Larkum, "A cellular mechanism for cortical associations: an organizing principle for the cerebral cortex," *Trends Neurosci.*, vol. 36, no. 3, pp. 141–151, 2013. doi: 10.1016/j.tins.2012.11.006
[7] Poirazi P, Brannon T, Mel B., Pyramidal Neuron as Two-Layer Neural Network, *Neuron*, 37, 989-999
[8] Markram H, Muller E, Ramaswamy S, et al., Reconstruction and Simulation of Neocortical Microcircuitry, *Cell*, 163, 456-492
[9] Poirazi, P., Papoutsi, A. Illuminating dendritic function with computational models. Nat Rev Neurosci 21, 303–321 (2020). https://doi.org/10.1038/s41583-020-0301-7
[10] Dehghani, N., Peyrache, A., Telenczuk, B. et al. Dynamic Balance of Excitation and Inhibition in Human and Monkey Neocortex. *Sci Rep* 6, 23176 (2016). https://doi.org/10.1038/srep23176
[11] Kubota Y, Karube F, Nomura M and Kawaguchi Y (2016) The Diversity of Cortical Inhibitory Synapses. *Front. Neural Circuits* 10:27. doi: 10.3389/fncir.2016.00027
[12] H. Ozeki, I. M. Finn, E. S. Schaffer, K. D. Miller, and D. Ferster, "Inhibitory stabilization of the cortical network underlies visual surround suppression," *Neuron*, vol. 62, no. 4, pp. 578–592, 2009
[13] C. Rössert et al., "Automated point-neuron simplification of data-driven microcircuit models," *arXiv preprint*, arXiv:1604.00087v2, 2017.
[14] Lagorce X et al. (2015) Breaking the millisecond barrier on SpiNNaker: implementing asynchronous event-based plastic models with microsecond resolution. *Front. Neurosci.* 9:206. doi: 10.3389/fnins.2015.00206
[15] C. R. Butson, S. E. Cooper, J. M. Henderson, and C. C. McIntyre, "Patient-specific analysis of the volume of tissue activated during deep brain stimulation," *NeuroImage*, vol. 34, no. 2, pp. 661–670, 2007
[16] NanoBanana, Google Gemini. “Basal ganglia circuit diagram”.
[17] Kiani, M.M., Heidari Beni, M.H. & Aghajan, H. Aberrations in temporal dynamics of cognitive processing induced by Parkinson’s disease and Levodopa. Sci Rep 13, 20195 (2023). https://doi.org/10.1038/s41598-023-47410-3

References

[1] W. Rall, "Membrane time constant of motoneurons," *Science*, vol. 126, p. 454, 1957.
[2] W. Rall, "Branching dendritic trees and motoneuron membrane resistivity," *Exp. Neurol.*, vol. 1, pp. 491–527, 1959.
[3] W. Rall, "Theory of physiological properties of dendrites," *Ann. N.Y. Acad. Sci.*, vol. 96, pp. 1071–1092, 1962.
[4] W. Rall, "Theoretical significance of dendritic trees for neuronal input-output relations," in *Neural Theory and Modeling*, 1964, pp. 73–97.
[5] M. London and M. Häusser, "Dendritic computation," *Annu. Rev. Neurosci.*, vol. 28, pp. 503–532, 2005.
[6] P. Poirazi, T. Brannon, and B. W. Mel, "Pyramidal neuron as two-layer neural network," *Neuron*, vol. 37, pp. 989–999, 2003.
[7] P. Poirazi, T. Brannon, and B. W. Mel, "Arithmetic of subthreshold synaptic summation in a model CA1 pyramidal cell," *Neuron*, vol. 37, pp. 977–987, 2003.
[8] A. Gidon et al., "Dendritic action potentials and computation in human layer 2/3 cortical neurons," *Science*, vol. 367, pp. 83–87, 2020.
[9] G. J. Stuart and N. Spruston, "Dendritic integration: 60 years of progress," *Nat. Neurosci.*, vol. 18, pp. 1713–1721, 2015.
[10] P. Poirazi and A. Papoutsi, "Illuminating dendritic function with computational models," *Nat. Rev. Neurosci.*, vol. 21, pp. 303–321, 2020.
[11] H. Markram et al., "Reconstruction and simulation of neocortical microcircuitry," *Cell*, vol. 163, pp. 456–492, 2015.
[12] E. Hay et al., "Models of neocortical layer 5b pyramidal cells...," *PLoS Comput. Biol.*, vol. 7, e1002107, 2011.
[13] N. W. Gouwens et al., "Classification of electrophysiological and morphological neuron types...," *Nat. Neurosci.*, vol. 22, pp. 1182–1195, 2019.
[14] N. W. Gouwens et al., "Integrated morphoelectric and transcriptomic classification...," *Cell*, vol. 183, pp. 935–953, 2020.
[15] G. A. Ascoli et al., "NeuroMorpho.Org...," *J. Neurosci.*, vol. 27, pp. 9247–9251, 2007.
[16] L. Kanari et al., "Objective morphological classification of neocortical pyramidal cells," *Cerebral Cortex*, vol. 29, pp. 1719–1735, 2019.
[17] M. V. Tsodyks and H. Markram, "The neural code between neocortical pyramidal neurons...," *PNAS*, vol. 94, pp. 719–723, 1997.
[18] H. Markram, Y. Wang, and M. Tsodyks, "Differential signaling via the same axon...," *PNAS*, vol. 95, pp. 5323–5328, 1998.
[19] M. Tsodyks, K. Pawelzik, and H. Markram, "Neural networks with dynamic synapses," *Neural Comput.*, vol. 10, pp. 821–835, 1998.
[20] R. S. Zucker and W. G. Regehr, "Short-term synaptic plasticity," *Annu. Rev. Physiol.*, vol. 64, pp. 355–405, 2002.
[21] L. F. Abbott and W. G. Regehr, "Synaptic computation," *Nature*, vol. 431, pp. 796–803, 2004.
[22] C. E. Jahr and C. F. Stevens, "A quantitative description of NMDA receptor-channel kinetic behavior," *J. Neurosci.*, vol. 10, pp. 1830–1837, 1990.
[23] C. E. Jahr and C. F. Stevens, "Voltage dependence of NMDA-activated macroscopic conductances...," *J. Neurosci.*, vol. 10, pp. 3178–3182, 1990.
[24] A. Destexhe, Z. F. Mainen, and T. J. Sejnowski, "Synthesis of models for excitable membranes...," *J. Comput. Neurosci.*, vol. 1, pp. 195–230, 1994.
[25] Y. Shu, A. Hasenstaub, and D. A. McCormick, "Turning on and off recurrent balanced cortical activity," *Nature*, vol. 423, pp. 288–293, 2003.
[26] M. Okun and I. Lampl, "Instantaneous correlation of excitation and inhibition...," *Nat. Neurosci.*, vol. 11, pp. 535–537, 2008.
[27] S. Denève and C. K. Machens, "Efficient codes and balanced networks," *Nat. Neurosci.*, vol. 19, pp. 375–382, 2016.
[28] R. J. Douglas and K. A. C. Martin, "A functional microcircuit for cat visual cortex," *J. Physiol.*, vol. 440, pp. 735–769, 1991.
[29] R. J. Douglas and K. A. C. Martin, "Neuronal circuits of the neocortex," *Annu. Rev. Neurosci.*, vol. 27, pp. 419–451, 2004.
[30] F. Pouille and M. Scanziani, "Enforcement of temporal fidelity...," *Science*, vol. 293, pp. 1159–1163, 2001.
[31] G. Silberberg and H. Markram, "Disynaptic inhibition between neocortical pyramidal cells...," *Neuron*, vol. 53, pp. 735–746, 2007.
[32] H. Ozeki et al., "Inhibitory stabilization of the cortical network...," *Neuron*, vol. 62, pp. 578–592, 2009.
[33] N. Brunel, "Dynamics of sparsely connected networks...," *J. Comput. Neurosci.*, vol. 8, pp. 183–208, 2000.
[34] H. R. Wilson and J. D. Cowan, "Excitatory and inhibitory interactions...," *Biophys. J.*, vol. 12, pp. 1–24, 1972.

References

[35] C. Rössert et al., "Automated point-neuron simplification of data-driven microcircuit models," arXiv:1604.00087v2, 2017.
[36] C. Pozzorini et al., "Automated high-throughput characterization of single neurons...," *PLoS Comput. Biol.*, vol. 11, e1004275, 2015.
[37] E. M. Izhikevich, "Simple model of spiking neurons," *IEEE Trans. Neural Netw.*, vol. 14, pp. 1569–1572, 2003.
[38] R. Brette and W. Gerstner, "Adaptive exponential integrate-and-fire model...," *J. Neurophysiol.*, vol. 94, pp. 3637–3642, 2005.
[39] C. Teeter et al., "Generalized leaky integrate-and-fire models classify multiple neuron types," *Nat. Commun.*, vol. 9, art. 709, 2018.
[40] S. Li et al., "Dendritic computations captured by an effective point neuron model," *PNAS*, vol. 116, pp. 15244–15252, 2019.
[41] W. Van Geit et al., "BluePyOpt...," *Front. Neuroinform.*, vol. 10, art. 17, 2016.
[42] M.-O. Gewaltig and M. Diesmann, "NEST (NEural Simulation Tool)," *Scholarpedia*, vol. 2, p. 1430, 2007.
[43] D. F. M. Goodman and R. Brette, "Brian: a simulator for spiking neural networks in Python," *Front. Neuroinform.*, vol. 2, art. 5, 2008.
[44] M. Stimberg, R. Brette, and D. F. M. Goodman, "Brian 2...," *eLife*, vol. 8, e47314, 2019.
[45] E. Yavuz, J. Turner, and T. Nowotny, "GeNN...," *Sci. Rep.*, vol. 6, art. 18854, 2016.
[46] A. P. Davison et al., "PyNN...," *Front. Neuroinform.*, vol. 2, art. 11, 2009.
[47] P. Kumbhar et al., "CoreNEURON...," *Front. Neuroinform.*, vol. 13, art. 63, 2019.
[48] S. B. Furber et al., "The SpiNNaker Project," *Proc. IEEE*, vol. 102, pp. 652–665, 2014.
[49] M. Davies et al., "Loihi: A neuromorphic manycore processor...," *IEEE Micro*, vol. 38, pp. 82–99, 2018.
[50] C. Pehle et al., "The BrainScaleS-2 accelerated neuromorphic system...," *Front. Neurosci.*, vol. 16, art. 795876, 2022.
[51] J. Schemmel et al., "A wafer-scale neuromorphic hardware system...," *Proc. IEEE ISCAS*, pp. 1947–1950, 2010.
[52] C. C. McIntyre et al., "Cellular effects of deep brain stimulation...," *J. Neurophysiol.*, vol. 91, pp. 1457–1469, 2004.
[53] C. C. McIntyre et al., "Uncovering the mechanism(s) of action of deep brain stimulation...," *Clin. Neurophysiol.*, vol. 115, pp. 1239–1248, 2004.
[54] W. M. Grill, A. N. Snyder, and S. Miocinovic, "Deep brain stimulation creates an informational lesion...," *NeuroReport*, vol. 15, pp. 1137–1140, 2004.
[55] C. R. Butson et al., "Patient-specific analysis of the volume of tissue activated...," *NeuroImage*, vol. 34, pp. 661–670, 2007.
[56] J. E. Rubin and D. Terman, "High frequency stimulation of the subthalamic nucleus...," *J. Comput. Neurosci.*, vol. 16, pp. 211–235, 2004.
[57] P. J. Hahn and C. C. McIntyre, "Modeling shifts in the rate and pattern...," *J. Comput. Neurosci.*, vol. 28, pp. 425–441, 2010.
[58] K. Kumaravelu, D. T. Brocker, and W. M. Grill, "A biophysical model of the cortex-basal ganglia-thalamus network...," *J. Comput. Neurosci.*, vol. 40, pp. 207–229, 2016.
[59] C. C. McIntyre and P. J. Hahn, "Network perspectives on the mechanisms of deep brain stimulation," *Neurobiol. Dis.*, vol. 38, pp. 329–337, 2010.
[60] S. Miocinovic et al., "History, applications, and mechanisms of deep brain stimulation," *JAMA Neurol.*, vol. 70, pp. 163–171, 2013.
[61] A. Horn et al., "Lead-DBS v2...," *NeuroImage*, vol. 184, pp. 293–316, 2019.
[62] J. E. Fleming, E. Dunn, and M. M. Lowery, "Simulation of closed-loop deep brain stimulation...," *Front. Neurosci.*, vol. 14, art. 166, 2020.
[63] J. E. Fleming et al., "Optimal closed-loop deep brain stimulation...," *PLoS Comput. Biol.*, vol. 17, e1009281, 2021.
[64] F. Rattay, "Analysis of models for external stimulation of axons," *IEEE Trans. Biomed. Eng.*, vol. 33, pp. 974–977, 1986.
[65] F. Rattay, "The basic mechanism for the electrical stimulation of the nervous system," *Neuroscience*, vol. 89, pp. 335–346, 1999.
[66] C. C. McIntyre and W. M. Grill, "Excitation of central nervous system neurons by nonuniform electric fields," *Biophys. J.*, vol. 76, pp. 878–888, 1999.
[67] C. C. McIntyre and W. M. Grill, "Extracellular stimulation of central neurons...," *J. Neurophysiol.*, vol. 88, pp. 1592–1604, 2002.
[68] G. R. Holt and C. Koch, "Electrical interactions via the extracellular potential near cell bodies," *J. Comput. Neurosci.*, vol. 6, pp. 169–184, 1999.
[69] Medtronic, "Medtronic earns U.S. FDA approval for the world's first Adaptive deep brain stimulation system for people with Parkinson's," Press Release, Feb. 24, 2025.
[70] G. Duffley, D. N. Anderson, J. Vorwerk, A. D. Dorval, and C. R. Butson, "Evaluation of methodologies for computing the deep brain stimulation volume of tissue activated," *J. Neural Eng.*, vol. 16, no. 6, art. 066024, 2019. doi: 10.1088/1741-2552/ab3c95